mathematics

MDPI

Article

Dynamical Behavior of a Fractional Order Model for Within-Host SARS-CoV-2

Kaushik Dehingia [1,*,†], Ahmed A. Mohsen [2,3,†], Sana Abdulkream Alharbi [4], Reima Daher Alsemiry [4] and Shahram Rezapour [5,6,*]

[1] Department of Mathematics, Sonari College, Sonari 785690, Assam, India
[2] Department of Mathematics, College of Education for Pure Science (Ibn Al-Haitham), University of Baghdad, Baghdad 10071, Iraq; aamuhseen@gmail.com
[3] Ministry of Education, Rusafa 1, Baghdad 10071, Iraq
[4] Department of Mathematics & Statistics, College of Science, Taibah University, Yanbu 41911, Almadinah Almunawarah, Saudi Arabia; saaharbi@taibahu.edu.sa (S.A.A.); rsumairi@taibahu.edu.sa (R.D.A.)
[5] Department of Mathematics, Azarbaijan Shahid Madani University, Tabriz 53751-71379, Iran
[6] Department of Medical Research, China Medical University Hospital, China Medical University, Taichung 404332, Taiwan
* Correspondence: kaushikdehingia17@gauhati.ac.in (K.D.); sh.rezapour@azaruniv.ac.ir or rezapourshahram@yahoo.ca (S.R.)
† These authors contributed equally to this work.

Abstract: The prime objective of the current study is to propose a novel mathematical framework under the fractional-order derivative, which describes the complex within-host behavior of SARS-CoV-2 by taking into account the effects of memory and carrier. To do this, we formulate a mathematical model of SARS-CoV-2 under the Caputo fractional-order derivative. We derived the conditions for the existence of equilibria of the model and computed the basic reproduction number $\mathcal{R}_0$. We used mathematical analysis to establish the proposed model's local and global stability results. Some numerical resolutions of our theoretical results are presented. The main result of this study is that as the fractional derivative order increases, the approach of the solution to the equilibrium points becomes faster. It is also observed that the value of $\mathcal{R}_0$ increases as the value of β and π_v increases.

Keywords: SARS-CoV-2; fractional order; local stability; global stability; basic reproduction number

MSC: 37M05; 37M10; 37N25; 92B05

Citation: Dehingia, K.; Mohsen, A.A.; Alharbi, S.A.; Alsemiry, R.D.; Rezapour, S. Dynamical Behavior of a Fractional Order Model for Within-Host SARS-CoV-2. *Mathematics* **2022**, *10*, 2344. https://doi.org/10.3390/math10132344

Academic Editors: Biao Tang and Xia Wang

Received: 15 May 2022
Accepted: 27 June 2022
Published: 4 July 2022

1. Introduction

In December 2019, coronavirus disease 2019 (COVID-19), which began in Wuhan, China, was classified as a global pandemic. Since then, it has rapidly spread throughout the world, becoming the most pressing public health crisis and affecting millions of people [1]. Severe acute respiratory syndrome coronavirus 2 (SARS-CoV-2) is responsible for this disease. SARS-CoV-2 is a single-stranded RNA virus with a positive-sense single-stranded RNA (+ssRNA) genome. SARS-CoV-2 is one of the viruses that belongs to the Coronaviridae family and the Nidovirales order [2]. In addition, SARS-CoV-2 belongs to the Beta coronavirus family, which includes two additional extremely deadly viruses, SARS-CoV and MERS-CoV [3]. COVID-19's infection dynamics are complicated by several factors, including uncertainty about the source of the infection, a long period of incubation during which an infected individual may not develop symptoms or be aware of their infection, and the inefficiency and lack of availability of drugs or vaccines. All of these factors contribute to the rapid spread of COVID-19, complicating disease control [4].

Mathematical modeling of diseases is a new research area in mathematical biology. Researchers have used mathematical modeling to observe the dynamics of disease spread in populations and the within-host dynamics in the body to control and manage disease

effects [5–8]. Several modeling studies on the spread, transmission, and infection dynamics of COVID-19 disease have been conducted in various regions. By fitting the data of four Chinese provinces, Hubei, Guangdong, Zhejiang, and Henan, Liang [3] proposed a mathematical framework to detect the rules of the spread of the following pneumonia illnesses: COVID-19, SARS, and MERS. According to their result, COVID-19 has a much faster growth rate than SARS and MERS. Yang and Wang et al. [4] formulated a mathematical model that incorporates an environmental reservoir along with non-constant transmission rates to investigate the outbreak of COVID-19 disease in Wuhan, China, and demonstrated their findings with publicly available data. The authors of [9] investigated a mathematical model for the COVID-19 outbreak in Wuhan, taking into account some key elements such as individual behavioral responses, governmental actions, zoonotic transmission, and mass emigration in a short period. Chen et al. [10] developed a mathematical framework to simulate SARS-CoV-2 phase-based transmissibility and reported that in Middle Eastern countries, the transmissibility of SARS-CoV-2 is higher than MERS, whereas it is lower than MERS in the Republic of Korea.

Fractional calculus has recently gained more attention in mathematical modeling due to it's salient features: fractional derivatives can capture memory effects due to their non-local nature and give a more realistic scenario than the integer-order differential model. In [11], the authors used Lagrange's interpolation method to analyze a fractal-fractional-order COVID-19 model and interpret their results numerically for various fractional orders. The optimal effects of physical distance on SARS-CoV-2 virus transmission were studied by Bushnaq et al. [12] using a fractional-order mathematical model. The researchers have considered control inputs such as social distancing and quarantine to minimize the number of susceptible and infected people while maximizing the number of people who can recover. Farman et al. [13] investigated a COVID-19 model using the Atangana–Baleanu fractional derivative and fractal-fractional Atangana–Baleanu with Mittag–Leffler kernel and derived a comparison analysis of the models with the considered fractional derivatives. Zhang et al. [14] simulated a new fractional-order mathematical model for the COVID-19 epidemic by employing the adaptive predictor-corrector algorithm and the fourth-order Runge–Kutta (RK4) method. To measure the spread of COVID-19, a SEIRD model was proposed by the authors in [15]. They estimated the parameters using both classical and fractional-order models fitted with data reported by WHO for Italy. It was observed that the root-mean-square error for the fractional-order model is lower than that of the classical one, and the fractional model provides a more accurate forecast of the data. In [16], a fractional-order model has been proposed to explore the effects of isolation, quarantine, and environmental viral load in the COVID-19 outbreak. Using data from Pakistan as input, they built a model and simulated the model using the Adams–Moulton scheme. Ahmad et al. [17] used the fractional-order derivative in Atangana–Baleanu sense to study a COVID-19 outbreak model for five different classes and fitted the model to data from Wuhan. A modified Adam–Bashforth method was used to arrive at an approximation of the numerical solution for this model. Moreover, one can find other works related to transmission dynamics of COVID-19 (see [18,19]).

A few modeling study works have been performed to understand the within-host behavior of SARS-CoV-2 dynamics. A mathematical model was proposed to demonstrate the within-host viral dynamics of SARS-CoV-2 such that the values of the parameters were estimated from score data of chest radiography, as shown in [20]. They also employed their mathematical model to analytically indicate the effect of drugs on virus growth and the immunity effect on patients. A few mathematical models were reviewed in [21] that are capable of explaining the dynamical behavior of SARS-CoV-2 and estimating the standard parameters of viral infections. Almocera et al. [22] explored the response of effector T cells to SARS-CoV-2 and gave a profound insight into how SARS-CoV-2 causes the disease by analyzing a within-host model. In [23], a comparative analysis of SARS-CoV-2 dynamics with that of MERS-CoV and SARS-CoV has been performed by investigating a quantitative model, which suggests that the infection of SARS-CoV-2 can be controlled if a combination therapy is used that triggers cytotoxicity and blocks de novo infection or virus production

synergistically. Vaidya et al. [24] characterized the dynamical infection of SARS-CoV-2 within the host in ferrets by investigating a mathematical model fitted with experimental data. Yin et al. [25] proposed a viral kinetic delay-differential model to assess the effects of T cells and antibodies on SARS-CoV-2 ineffectiveness in patients with various symptoms. Afonyushkin et al. [26] investigated the distribution of the SARS-CoV-2 virus in human tissue and organs using a multi-compartmental model. Recently, Nath et al. [27] discussed the dynamical behavior of the model that was introduced by Li et al. [20]. This study aims to modify the model considered by Nath et al. [27] to a fractional-order one for understanding the complex behavior of SARS-CoV-2 in the host.

The remaining parts of the paper are assembled as follows: A fractional-order model that describes the dynamics of SARS-CoV-2 has been formulated in Section 2. Section 3 deals with a few preliminary concepts related to fractional calculus. The model has been analyzed by presenting the equilibrium points, stability analysis, and global stability analysis in Sections 4–6. A numerical simulation of the model has been performed in Section 7. Finally, concluding remarks of the paper have been presented in Section 8.

2. Formulation of COVID-19 Model

2.1. The Original COVID-19 Model

The original model [20,27] consists of three classes that categorize individuals with respect to the within-host coronavirus disease based on their status, as indicate in Figure 1. The class $M_p(t)$ represents virus-free pulmonary epithelial cells, the virus-infected pulmonary cells are represented by the class $M_p^*(t)$, and the class $v(t)$ represents the free virus. In addition, d_M, d_{M^*}, and d_v are the death rates of classes $M_p(t)$, $M_p^*(t)$, and $v(t)$, respectively. The transmission rate from virus-free cells to virus-infected cells is denoted by β. The free virus production rate is π_v. In the following model, the constant regeneration rate of $v(t)$ will be described by the term $d_M M_p(0)$.

$$\begin{cases} M_p(t) = d_M(M_p(0) - M_p(t)) - \beta M_p(t)v(t), \\ M_p^*(t) = \beta M_p v(t) - d_{M^*} M_p^*(t), \\ v(t) = \pi_v M_p^*(t) - d_v v(t). \end{cases} \tag{1}$$

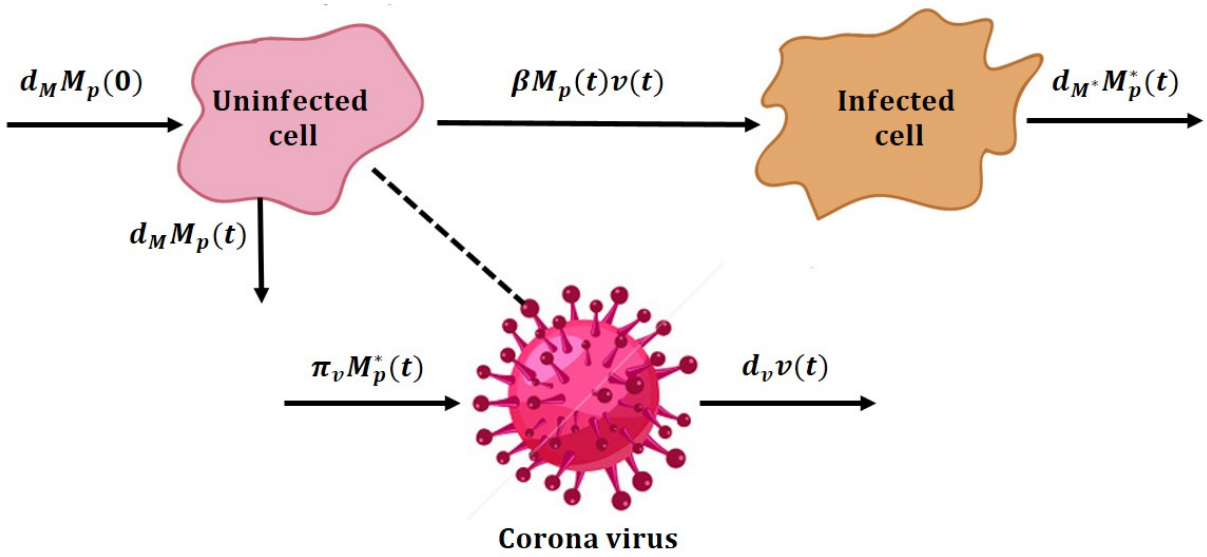

Figure 1. Schematic diagram of the model (1).

2.2. The Fractional COVID-19 Model

For the model's modification by the general (M_p, M_p^*, v) within-host coronavirus model (1), we can express the following fractional within-host coronavirus model:

$$\begin{cases} D^{\alpha} M_p(t) = d_M(M_p(0) - M_p(t)) - \beta M_p(t)v(t), \\ D^{\alpha} M_p^*(t) = \beta M_p(t)v(t) - d_{M^*} M_p^*(t), \\ D^{\alpha} v(t) = \pi_v M_p^*(t) - d_v v(t), \end{cases} \tag{2}$$

with the initial conditions

$$M_p(0) > 0, \quad M_p^*(0) \geq 0 \quad and \quad v(0) \geq 0. \tag{3}$$

Here, D^{α} is the fractional Caputo derivative with α order as $\alpha \in (0, 1]$ that indicates the memory effects in the proposed $M_p M_p^* v$ within-host coronavirus model. We consider that the functions $M_p(t), M_p^*(t), v(t)$ with their Caputo fractional derivative order as $\alpha \in (0, 1]$ are continuous functions. All the parameters in the fractional-order model (2) are within the interval $(0, 1]$ and the values are taken from [20,27] that were used in analysis of model (1).

3. Preliminaries of Fractional-Order Derivative

This section reviews the fundamental definitions, theorems, concepts, and results that we will use throughout the remainder of this paper. For more details, we refer the reader to [28–31].

Definition 1. *The fractional-order derivative in Caputo sense for order $x > 0$ is defined below:*

$$D_t^x f(t) = \frac{1}{\Gamma(n-x)} \int_a^t (t-\xi)^{n-x-1} f^{(n)}(\xi) d\xi,$$

where $n - 1 < x \leq n$, $n \in N$, $f \in C^{n-1}[0, t]$.

Definition 2. *The Atangana–Baleanu Caputo fractional derivative for a given function for order x is defined below:*

$$D_t^x f(t) = \frac{B(x)}{1-x} \int_a^t \frac{df(\xi)}{d\xi} E_x[-\frac{x}{1-x}(t-\xi)^x] d\xi,$$

where $B(x) = (1-x) + \frac{x}{\Gamma(x)}$ is a normalization function and $E_{\alpha}(.)$ is the Mittag–Leffler function.

Definition 3. *An integral order x under the Atangana–Baleanu fractional derivative is defined by*

$$I_t^x(f(t)) = \frac{1-x}{B(x)} f(t) + \frac{x}{B(x)\Gamma(x)} \int_a^t f(\xi)(t-\xi)^{x-1} d\xi,$$

and the integral will be zero for a constant function $f(t)$.

Definition 4. *The Laplace transform for the Atangana–Baleanu fractional operator of order x is computed as follows:*

$$LD^x f(t)(s) = \frac{B(x)}{1-x} \frac{S^x Lf(t)(s) - s^{x-1} f(a)}{s^x + \frac{x}{1-x}}, \quad where\ x \in (0, 1].$$

Definition 5. *The function f satisfies the Hölder continuous function if and only if there are $C, v \in \Re^+$ constants such that $||f(x) - f(y)|| \leq C||x - y||^v$.*

Lemma 1. *Let the system be $D^{\theta} x(t) = \phi(t, x)$, where $\phi : [t_0, \infty) \times \Omega \to \Re^m, \Omega \subseteq \Re^m$, $t > t_0$, and $0 < \theta \leq 1$ with $x(t_0)$ as the initial condition. Then, for the above system, there exists a unique solution on $[t_0, \infty) \times \Omega$ if the Lipschitz condition with respect to x holds for $\phi(t, x)$.*

Lemma 2. *Let a nonlinear fractional-order system be* $D_t^\theta x = \phi(x)$, *where* $x(t_0) = x_0$ *and* $0 < \theta < 1$. *If a point* x^* *satisfies* $\phi(x^*) = 0$, *then* x^* *is called an equilibrium point of the system. The equilibrium* x^* *is said to be locally asymptotically stable if all eigenvalues* λ_i *of the Jacobian matrix* $J = \frac{\partial \phi}{\partial x}$ *evaluated at* x^* *satisfy the conditions* $|arg(\lambda_i)| > \frac{\theta\pi}{2}$.

Lemma 3. *Let* $D_t^\theta x = \phi(t, x)$ *be a system with* $x(t_0) = x_0$, $0 < \theta < 1$, *such that* $\phi(t, x)$ *is a continuous function in* x *and locally Lipschitz in* x. *Thus,* $\forall t > 0$, $\exists x(t) \in \Omega$ *such that* $v \in C^{0,v}$ *with* $\theta < v < 0$ *be a locally Hölder continuous function such that*

$$D_t^\theta v \leq f(t, (v(t)), v(0) \leq x(0) \Rightarrow v(t) \leq x(t)\ \forall t \in [0, T).$$

Lemma 4 ([32,33])**.** *Suppose that* Ω *is a bounded closed set. Every solution of* $D_t^\theta x(t) = f(x)$ *starts from a point in* Ω *and remains in* Ω *for all time. If* $\exists\ \phi(x) : \Omega \to \mathbb{R}$ *with continuous first partial derivatives satisfies the following condition,*

$$D_t^\theta(\phi)|_{D_t^\theta x(t) = f(x)} \leq 0.$$

If $E = \{x, D_t^\theta(\phi)|_{D_t^\theta x(t) = f(x)} = 0\}$ *and* M *is the largest invariant set of* E, *then every solution* $x(t)$ *originating in* Ω *tends to* M *as* $t \to \infty$. *Specifically, when* $M = \{0\}$, *then* $x \to 0$, *as* $t \to \infty$.

4. Analysis of the Model

The evaluation of the equilibrium of the model (2) is done by finding all the possible roots of the model (2) when all fractional derivatives in the model (2) are equal to zero:

$$\mathcal{D}^\alpha M_p(t) = \mathcal{D}^\alpha M_p^*(t) = \mathcal{D}^\alpha v(t) = 0 \to M_p, M_p^*, v \equiv \text{constants}, \tag{4}$$

which gives

$$\begin{aligned} 0 &= d_M(M_p(0) - M_p) - \beta M_p v, \\ 0 &= \beta M_p v - d_{M^*} M_p^*, \\ 0 &= \pi_v M_p^* - d_v v. \end{aligned} \tag{5}$$

The uninfected equilibrium (UIE) of the model (2) can be computed by solving the system (5) and given by the form $e_1 = (M_p(0), 0, 0)$.

Furthermore, the model (2) can be written as

$$\frac{dX}{dt} = \mathcal{F}(x) - \varphi(t), \tag{6}$$

where

$$X(t) = \begin{pmatrix} M_p^* \\ M_p(t) \\ v(t) \end{pmatrix}, \mathcal{F}(x) = \begin{pmatrix} \beta M_p v \\ 0 \\ 0 \end{pmatrix}, \tag{7}$$

$$\varphi(t) = \begin{pmatrix} d_{M^*} M_p^* \\ -d_M(M_p(0) - M_p) + \beta M_p v \\ -\pi_v M_p^* + d_v v \end{pmatrix}, \tag{8}$$

and then we have

$$F = \left[\frac{\partial \mathcal{F}_i}{\partial x_j}(x_0)\right] = \begin{pmatrix} 0 & 0 & \beta M_p(0) \\ 0 & 0 & 0 \\ 0 & 0 & 0 \end{pmatrix}, \tag{9}$$

$$
\begin{aligned}
V &= \left[\frac{\partial \varphi_i}{\partial x_j}(x_0)\right] \\
&= \begin{pmatrix} d_{M_p^*} & 0 & 0 \\ 0 & \frac{d_M(\pi_v \beta M_p(0) - d_{M_p^*} d_v)}{d_{M_p^*} d_v} + d_M & \frac{d_{M_p^*} d_v}{\pi_v} \\ -\pi_v & 0 & d_v \end{pmatrix},
\end{aligned} \tag{10}
$$

$$
FV^{-1} = \begin{pmatrix} \frac{\beta M_p(0)\pi_v}{d_{M^*} d_v} & 0 & \frac{\beta M_p(0)}{d_v} \\ 0 & 0 & 0 \\ 0 & 0 & 0 \end{pmatrix}, \tag{11}
$$

where the matrix (11) is called the next-generation matrix for the model and $\mathcal{R}_0 = \frac{\beta M_p(0)\pi_v}{d_{M^*} d_v}$.

Lemma 5. *There exists a unique virus-infected equilibrium point (VIE) of model (2)* $e_2 = (M_p, M_p^*, v)$ *if and only if* $\mathcal{R}_0 > 1$.

Proof. A virus-infected equilibrium of the model (2) is exists, if the following equations are satisfying:

$$
\begin{aligned}
d_M(M_p(0) - M_p) - \beta M_p v &= 0, \\
\beta M_p v - d_{M^*} M_p^* &= 0, \\
\pi_v M_p^* - d_v v &= 0.
\end{aligned} \tag{12}
$$

It is straightforward to calculate that there exists a unique solution to (12) that satisfies

$$
\begin{aligned}
M_p &= \frac{d_{M^*} d_v}{\pi_v \beta} = M_p(0)\frac{1}{\mathcal{R}_0}, \\
M_p^* &= \frac{d_v v}{\pi_v} = \frac{d_v d_M}{\beta \pi_v}(\mathcal{R}_0 - 1), \\
v &= \frac{d_M}{\beta}(\mathcal{R}_0 - 1).
\end{aligned} \tag{13}
$$

Obviously, $M_p > 0$, where $\frac{d_{M^*} d_v}{\pi_v \beta} > 0 \ \forall t$, but $M_p^* > 0$ and $v > 0$ are hold if and only if $\mathcal{R}_0 > 1$. Hence, the virus-infected equilibrium point of the model (2) can be computed as $e_2 = (M_p(0)\frac{1}{\mathcal{R}_0}, \frac{d_v d_M}{\beta \pi_v}(\mathcal{R}_0 - 1), \frac{d_M}{\beta}(\mathcal{R}_0 - 1))$ and it exists if and only if $\mathcal{R}_0 > 1$. □

5. Local Stability

Herein, the local stability analysis will be discussed near all equilibrium points of model (2) through the following theorems.

Theorem 1. *Suppose that* $g : \Omega \subset \Re_+^3 \to \Re_+^3$ *is a differentiable function and* $e_1 \in \Omega$*; then, uninfected equilibrium point* e_1 *is locally asymptotically stable if the following condition holds:*

$$
\pi_v \beta M_p(0) < d_{M^*} d_v. \tag{14}
$$

Otherwise, it becomes unstable.

Proof. The Jacobian matrix at uninfected equilibrium point e_1 can be written as

$$J(e_1) = \begin{pmatrix} -d_M & 0 & -\beta M_p(0) \\ 0 & -d_{M^*} & \beta M_p(0) \\ 0 & \pi_v & -d_v \end{pmatrix}. \tag{15}$$

Clearly, the characteristic equation of the above matrix $J(e_1)$ is

$$(-d_M - \lambda)(\lambda^2 + T\lambda + D) = 0, \tag{16}$$

and here,

$$T(trace) = d_{M^*} + d_v > 0,$$
$$D(determent) = d_{M^*}d_v - \pi_v\beta M_p(0).$$

Now, if the condition (14) is satisfied, we find that the uninfected equilibrium point e_1 is locally asymptotically stable. □

Theorem 2. *The virus-infected equilibrium point e_2, is locally asymptotically stable whenever*

$$\pi_v\beta\bar{M}_p \leq d_v d_{M^*}. \tag{17}$$

Proof. The Jacobian matrix at the virus-infected equilibrium point e_2 can be written as

$$J(e_2) = \begin{pmatrix} -(d_M + \beta\bar{v}) & 0 & -\beta\bar{M}_p \\ \beta\bar{v} & -d_{M^*} & \beta\bar{M}_p \\ 0 & \pi_v & -d_v \end{pmatrix}. \tag{18}$$

The characteristic equation of the above matrix $J(e_2)$ is

$$\lambda^3 + A_1\lambda^2 + A_2\lambda + A_3 = 0, \tag{19}$$

where

$$A_1 = d_M + \beta\bar{v} + d_{M^*} + d_v,$$

$$A_2 = (d_M + \beta\bar{v})(d_v + d_{M^*}) + d_{M^*}d_v - \pi_v\beta\bar{M}_p,$$

$$A_3 = (d_M + \beta\bar{v})(d_v d_{M^*} - \pi_v\beta\bar{M}_p) + \pi_v\beta^2\bar{v}\bar{M}_p,$$

$$\begin{aligned} A_1A_2 - A_3 = {} & d_{M^*}(d_M + \beta\bar{v})[d_M + \beta\bar{v} + d_{M^*}] \\ & + d_v(d_M + \beta\bar{v})(d_M + \beta\bar{v} + d_v) \\ & + \pi_v\beta^2\bar{v}\bar{M}_p - (d_v + d_{M^*})\times \\ & (\pi_v\beta\bar{M}_p - d_v d_{M^*}) \\ & - 2(d_M + \beta\bar{v})(\pi_v\beta\bar{M}_p - 2d_v d_{M^*}). \end{aligned}$$

Thus, under both conditions $\mathcal{R}_0 > 1$ and (17), we have A_i, which are positive, where $i = 1, 2, 3$ and $A_1A_2 - A_3 > 0$, and hence, according to the Routh–Hurwitz criterion, the virus-infected equilibrium point e_2 is locally asymptotically stable. □

6. Global Stability

Herein, the global stability of the system (2) will be discussed through the following theorems.

Theorem 3. *The uninfected equilibrium point e_1 is globally asymptotically stable on the domain if and only if $\mathcal{R}_0 < 1$.*

Proof. By assuming the change $\mathcal{X}(t) = M_p(t) - M_p(0)$, the model (2) is equivalent to the following model:

$$\begin{cases} D^{\alpha}\mathcal{X}(t) = -d_M\mathcal{X}(t) - \beta\mathcal{X}(t)v(t) - \beta M_p(0)v(t), \\ D^{\alpha}M_p^*(t) = \beta\mathcal{X}(t)v(t) + \beta M_p(0)v(t) - d_{M^*}M_p^*(t), \\ D^{\alpha}v(t) = \pi_v M_p^*(t) - d_v v(t). \end{cases} \tag{20}$$

Hence, it clear to investigate that

$$\begin{cases} -d_M\mathcal{X}(t) - \beta\mathcal{X}(t)v(t) - \beta M_p(0)v \leq -d_M\mathcal{X}(t) - \beta M_p(0)v(t), \\ \beta\mathcal{X}(t)v(t) + \beta M_p(0)v(t) - d_{M^*}M_p^*(t) \leq \beta M_p(0)v(t) - d_{M^*}M_p^*(t), \\ \pi_v M_p^*(t) - d_v v(t) \leq -d_v v(t). \end{cases} \tag{21}$$

From (21), the solutions of the model (20) satisfy the following differential inequality:

$$\begin{cases} D^{\alpha}\mathcal{X}(t) \leq -d_M\mathcal{X}(t) - \beta M_p(0)v(t), \\ D^{\alpha}M_p^*(t) \leq \beta M_p(0)v(t) - d_{M^*}M_p^*(t), \\ D^{\alpha}v(t) \leq -d_v v(t). \end{cases} \tag{22}$$

By assuming that $(x(t), e_p^*(t), \nu(t))$ is a solution of the following linear fractional model,

$$\begin{cases} D^{\alpha}x(t) = -d_M x(t) - \beta M_p(0)\nu(t), \\ D^{\alpha}e_p^*(t) = \beta M_p(0)v(t) - d_{M^*}M_p^*(t), \\ D^{\alpha}\nu(t) = -d_v\nu(t). \end{cases} \tag{23}$$

such that the initial condition is given by $(x(0), e_p^*(0), \nu(0))$. Thus, the eigenvalues of the system (23) can be evaluated as

$$\begin{vmatrix} -d_M - \lambda & 0 & -\beta M_p(0) \\ 0 & -d_{M^*} - \lambda & \beta M_p(0) \\ 0 & 0 & -d_v - \lambda \end{vmatrix} = (-d_M - \lambda)(-d_{M^*} - \lambda)(-d_v - \lambda) = 0.$$

Clearly, $\lambda_i < 0$, where $i = 1, 2, 3$. Thus, $|arg(\lambda_i)| = \pi, i = 1, 2, 3$. From Lemma 2, we find that $\lim_{t\to\infty} x(t) = 0$, $\lim_{t\to\infty} e(t) = 0$ and $\lim_{t\to\infty} \nu(t) = 0$. Furthermore, by using Lemma 3, we find that

$$(\mathcal{X}(t), M_p^*(t), v(t)) < (x(t), e(t), \nu(t)) \Rightarrow \lim_{t\to\infty}(\mathcal{X}(t), M_p^*(t), v(t)) = (0, 0, 0),$$

and followed by this, we obtain

$$(M_p(t), M_p^*(t), v(t)) \to e_1.$$

Thus, the uninfected equilibrium point e_1 is globally asymptotically stable on the domain. □

Lemma 6. *Assume that there is a continuous and differentiable function $x(t) \in \Re^+$ such that $\forall\ t \geq t_0$ and $0 < \alpha < 1$; we have*

$$D_t^{\alpha}[(x(t) - a\ln x(t)] \leq (1 - \frac{a}{x(t)})D_t^{\alpha}x(t), a \in \Re^+.$$

Theorem 4. *The virus-infected equilibrium point e_2 of the model (2) is globally stable on the domain if and only if $\mathcal{R}_0 > 1$.*

Proof. Let $U : \Omega \subset \Re_+^3 \to \Re_+$; the Lyapunov function is given by

$$U(M_p, M_p^*, v) = (M_p - \bar{M}_p \ln M_p) + (M_p^* - \bar{M}_p^* \ln M_p^*) + (v - \bar{v}\ln v).$$

From Lemma 6, we have

$$\begin{aligned} D_t^{\alpha} U(M_p, M_p^*, v) &\leq \frac{M_p - \bar{M}_p}{M_p} D_t^{\alpha} M_p(t) + \frac{M_p^* - \bar{M}_p^*}{M^*{}_p} D_t^{\alpha} M_p^*(t) + \frac{v - \bar{v}}{v} D_t^{\alpha} v(t) \\ &= \frac{M_p - \bar{M}_p}{M_p}(d_M(M_p(0) - M_p) - \beta M_p v) + \frac{M_p^* - \bar{M}_p^*}{M^*{}_p}(\beta M_p v - d_{M^*} M_p^*) \\ &+ \frac{v - \bar{v}}{v}(\pi_v M_p^* - d_v v). \end{aligned}$$

From the equations at e_2, we have

$$\begin{aligned} -d_M &= \beta\bar{v} - \frac{d_M M_p(0)}{\bar{M}_p}, \\ -d_{M^*} &= -\frac{\beta \bar{M}_p \bar{v}}{\bar{M}_p^*}, \\ -d_v &= -\frac{\pi_v \bar{M}_p^*}{\bar{v}}. \end{aligned}$$

Hence,

$$\begin{aligned} D_t^{\alpha} U(M_p, M_p^*, v) &\leq -\frac{d_M M_P(0)}{M_p \bar{M}_p}(M_P - \bar{M}_p)^2 \\ &- \left(\frac{(\pi M_p^* + \beta \bar{M}_p v)\bar{v}}{v} + \frac{(\pi M_p^* + \beta \bar{M}_p \bar{v}) v \bar{M}_p^*}{M_p^* \bar{v}} + \frac{\beta \bar{M}_p (M_p \bar{v} + v \bar{M}_p^*)}{\bar{M}_p^*}\right) \\ &+ \pi(M_p + \bar{M}_p^*) + 2\beta(M_p v + \bar{M}_p \bar{v}) \\ &< 0. \end{aligned} \tag{24}$$

The inequality (24) is satisfied if and only if

$$\begin{aligned} &- \frac{d_M M_P(0)}{M_p \bar{M}_p}(M_P - \bar{M}_p)^2 \\ &- \left(\frac{(\pi M_p^* + \beta \bar{M}_p v)\bar{v}}{v} + \frac{(\pi M_p^* + \beta \bar{M}_p \bar{v}) v \bar{M}_p^*}{M_p^* \bar{v}} + \frac{\beta \bar{M}_p (M_p \bar{v} + v \bar{M}_p^*)}{\bar{M}_p^*}\right) \\ &> \pi(M_p + \bar{M}_p^*) + 2\beta(M_p v + \bar{M}_p \bar{v}). \end{aligned}$$

By using Lemma 4, we can deduce that the virus-infected equilibrium point e_2 is the largest invariant set containing all bounded solutions in Ω. Thus, the proof is completed. □

7. Numerical Simulation

In this section, to confirm the theoretical results obtained in the previous sections, we provide a numerical simulation for the solution of the model (2) under the fractional-order effect. In Figure 2, we show the results obtained as α changes between $\{1, 0.9, 0.4, 0.3\}$. The initial conditions $M_p(0) = 22.41, M_p^*(0) = 2.59, v(0) = 0.061$. The parameters $d_M = 0.3, \beta = 0.001, d_{M^*} = 0.11, \pi_v = 0.24, d_v = 0.26$. This implies that $\mathcal{R}_0 = 0.84 < 1$ and the solution of model (2) converge to uninfected equilibrium point e_1. Meanwhile, in Figure 3, if the transmission rate (β) increases from (0.001 to 0.01) with the same α values, we obtain the uninfected equilibrium point, which becomes unstable, and the solution of model (2) converges to the virus-infected equilibrium point e_2 and $\mathcal{R}_0 = 8.4 > 1$.

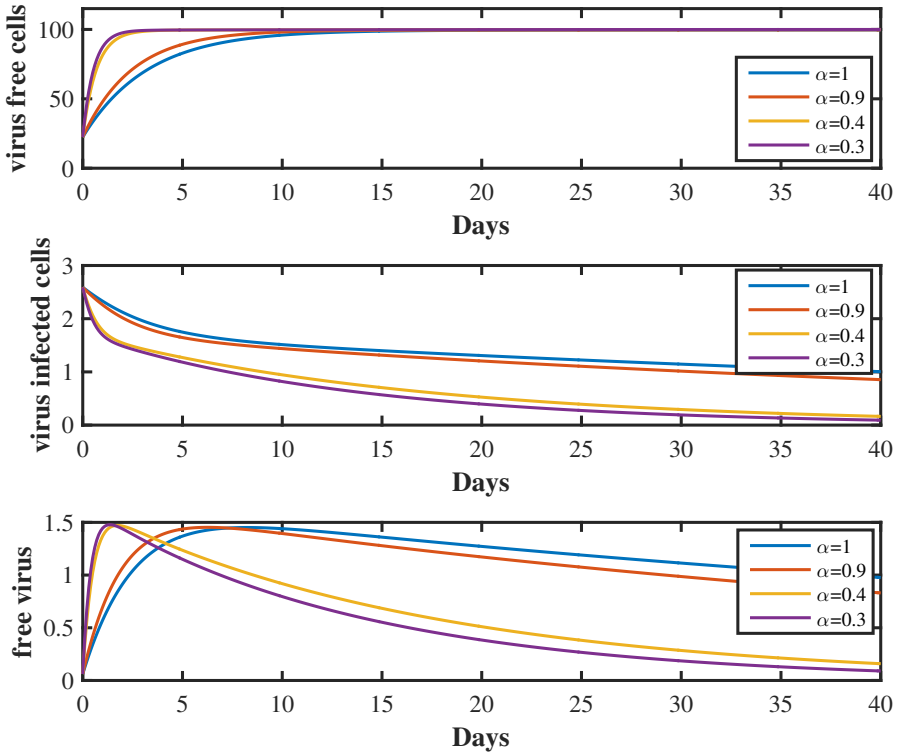

Figure 2. Numerical solution of the model (2) under different α values.

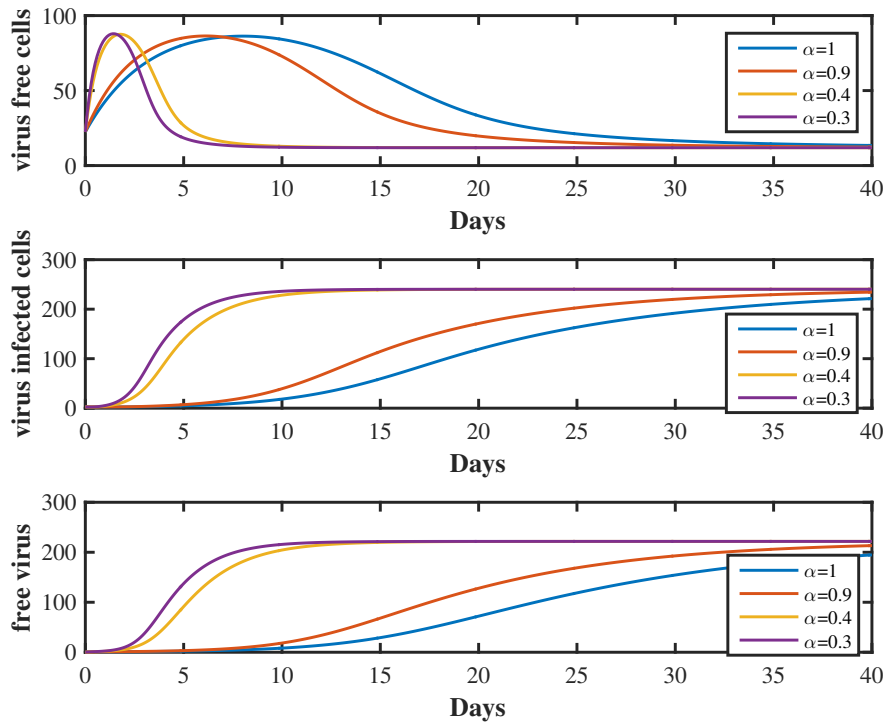

Figure 3. Numerical solution of the model (2) under different α values.

In Figure 4, we use the same initial condition and data but fix $\alpha = 0.9$ with different values of β. We find that the number of virus-free cells decreases and all numbers of virus-infected cells and virus-free cells increases, while the solution of the model (2) approaches e_2, which means that the e_1 becomes unstable.

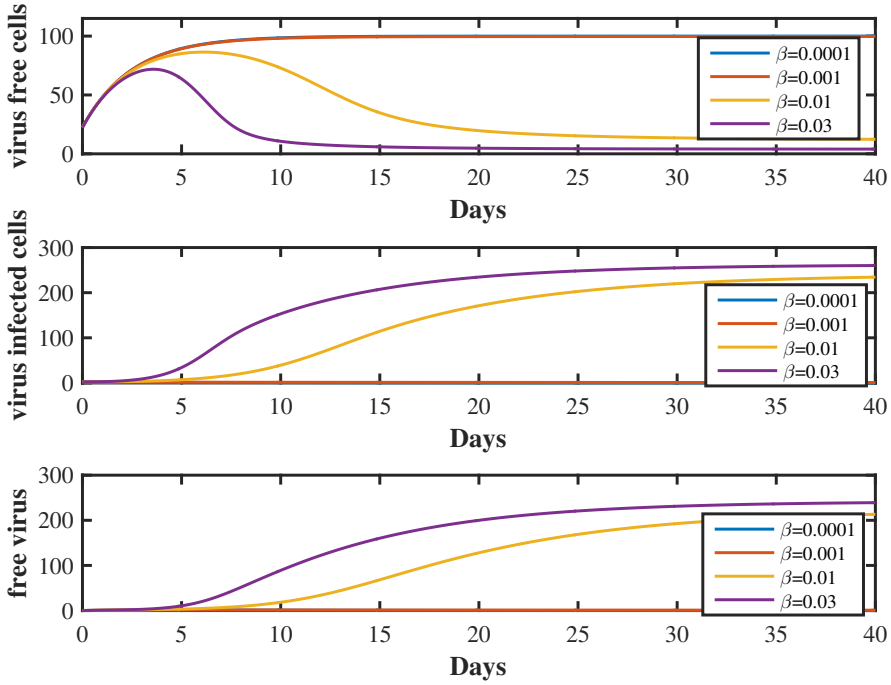

Figure 4. Numerical solution of the model (2) when fixing $\alpha = 0.9$ and with different β values.

In Figure 5, we use the same initial condition and data but fix $\alpha = 0.4$ with different values of π_v. We find that the number of virus-free cells decreases and all numbers of the virus-infected cells and virus-free cells increases, while the solution of the model (2) approaches e_2, which means that the e_1 becomes unstable.

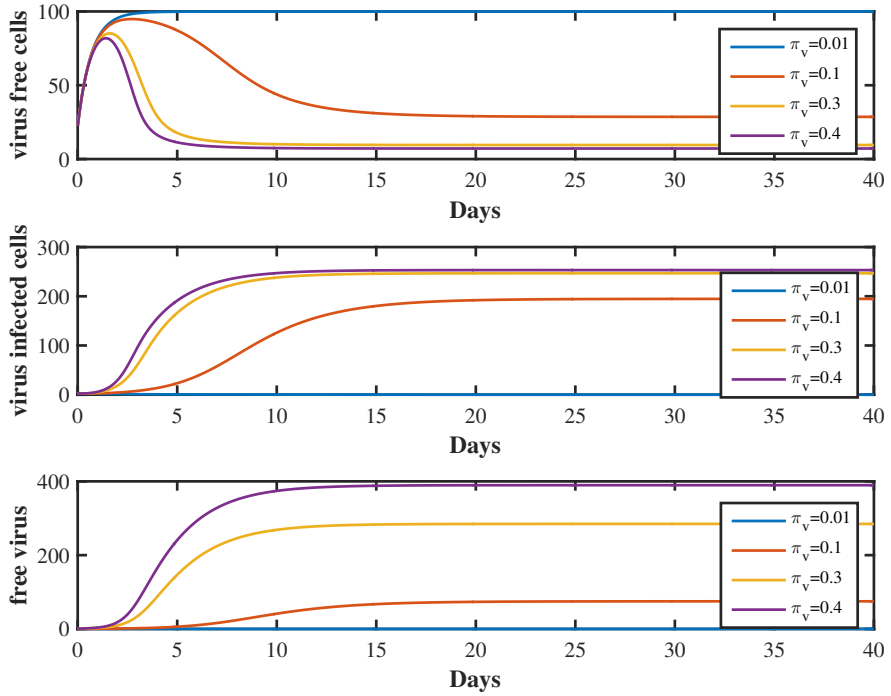

Figure 5. Numerical solution of the model (2) when fixing $\alpha = 0.4$ and with different π_v values.

8. Conclusions

Epidemiological models play a basic role in constructing strategies for understanding, preventing, and controlling infectious diseases through vaccination, social distancing

between individuals, quarantine, and wearing masks. This paper presents an epidemiological model of within-host SARS-CoV-2 transmission dynamics under the fractional-order derivative effect. Firstly, the existence, non-negativity, and bounds of the solution of the model are discussed. It is obtained that the model has two equilibrium points, namely the non-infected point and the virus-infected point. The explicit expression for the effective reproduction number $\mathcal{R}_0$, which gives the actual number of infections to infectious cells at any time, is found. The dynamical behavior of the system concerning $\mathcal{R}_0$ is investigated. It is observed that the non-infected equilibrium is globally stable if $\mathcal{R}_0 < 1$. The system persistence near the virus-infected equilibrium when $\mathcal{R}_0 < 1$ is discussed. From the obtained numerical simulation results, it is observed that as the fractional order derivative increases, the approach of the solution to the equilibrium points becomes faster. This paper uses the Caputo fractional-order derivative operator to form a fractional-order mathematical model of the spread of within-host SARS-CoV-2. The transmission rate effect on the dynamical behavior with a fixed value of the fractional order is studied. It is obtained that the system solution approaches the virus-infected equilibrium point. Hence, the value of $\mathcal{R}_0$ increases as β increases (see Figure 6). The effect of increasing the virus production rate on the dynamical behavior is studied, in addition, by using different values for the fixed value of the fractional order. It is observed that the value of $\mathcal{R}_0$ increases as π_v increases (see Figure 7).

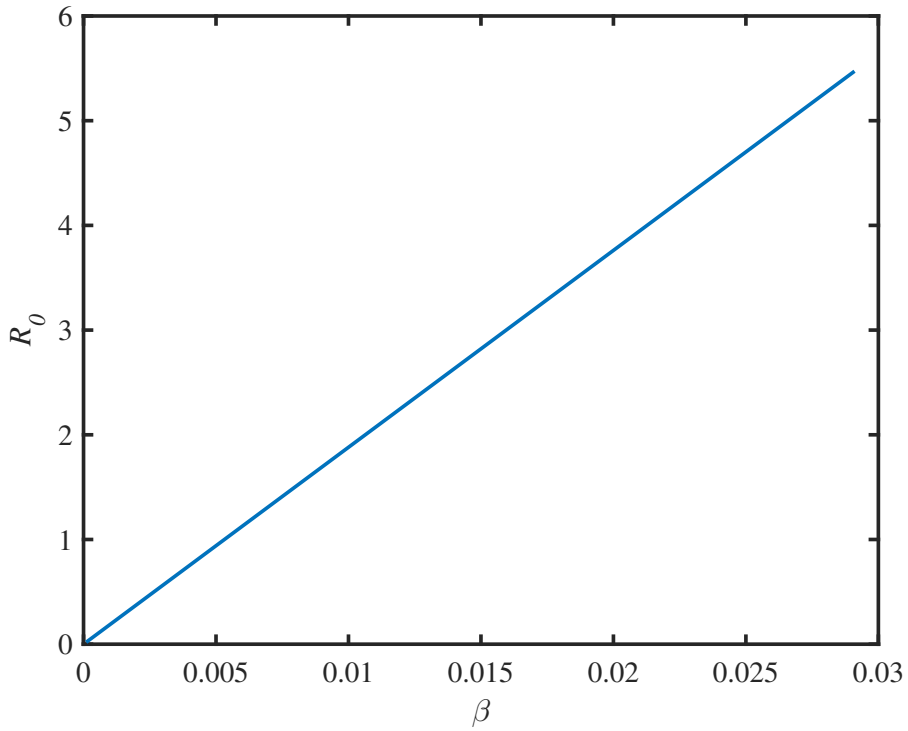

Figure 6. The positive relationship between R_0 and β.

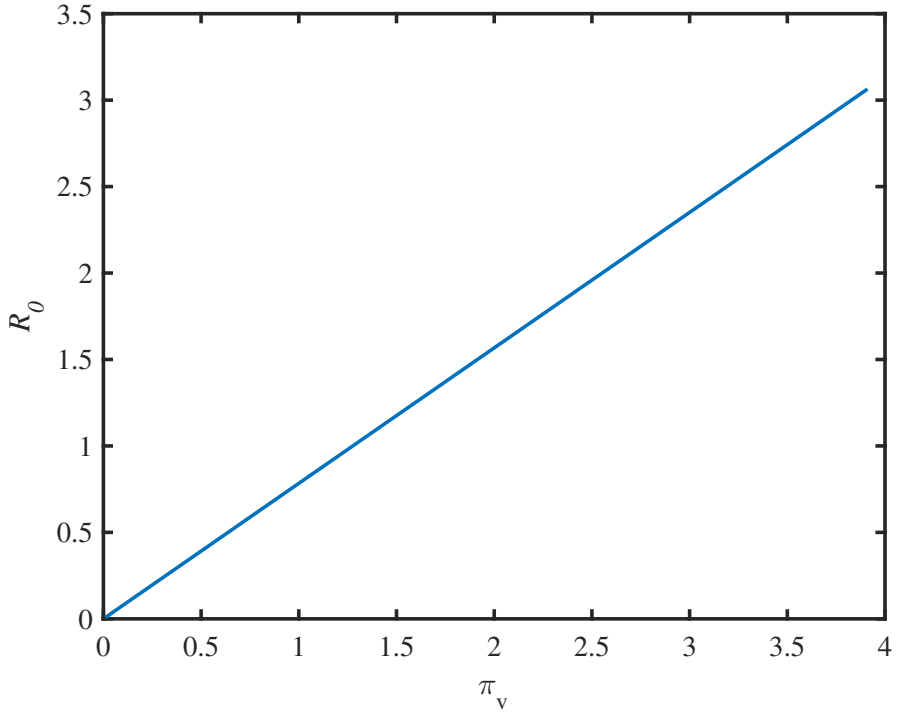

Figure 7. The positive relationship between R_0 and π_v.

It will be interesting to consider the impact of the vaccine with and without time delay for further work. Vaccination is one of the most effective methods of mitigation and elimination during epidemics, as evidenced in such epidemics as hepatitis, poliomyelitis, and, most recently, COVID-19. Moreover, the model can be further extended to an optimal one by choosing control parameters with which the disease can be controlled. In this regard, the authors would like to suggest a few works [34–36] that are related to optimal control concepts. Moreover, in the present study, we only discussed the local and global stability of the considered model. While analysis of a fractional-order system, the Ulam-Hyers stability (which guarantees a close exact solution to the system) is also an essential topic [37–39], and it will be considered in our future work.

Author Contributions: Conceptualization and methodology, K.D. and A.A.M.; software, A.A.M. and K.D.; validation, K.D., A.A.M., S.A.A. and R.D.A.; formal analysis, K.D., A.A.M., S.A.A. and R.D.A.; writing—original draft preparation, K.D., A.A.M. and S.A.A.; writing—review and editing, K.D. and S.A.A.; supervision, K.D. and S.R. All authors jointly worked on the results and they read and approved the final manuscript.

Funding: This research received no external funding.

Institutional Review Board Statement: Not applicable.

Informed Consent Statement: Not applicable.

Data Availability Statement: Not applicable.

Conflicts of Interest: The authors declare that they have no competing interests.

References

1. Du, S.Q.; Yuan, W. Mathematical modeling of interaction between innate and adaptive immune responses in COVID-19 and implications for viral pathogenesis. *J. Med. Virol.* **2020**, 92, 1615–1628. [CrossRef] [PubMed]
2. Harapan, H.; Itoh, N.; Yufika, A.; Winardi, W.; Keam, S.; Te, H.; Megawati, D.; Hayati, Z.; Wagner, A.L.; Mudatsir, M. Coronavirus disease 2019 (COVID-19): A literature review. *J. Infect. Public Health* **2020**, *13*, 667–673. [CrossRef] [PubMed]
3. Liang, K. Mathematical model of infection kinetics and its analysis for COVID-19, SARS and MERS. *Infect. Genet. Evol.* **2020**, *82*, 104306. [CrossRef] [PubMed]

4. Yang, C.; Wang, J. A mathematical model for the novel coronavirus epidemic in Wuhan, China. *Math. Biosci. Eng.* **2020**, *17*, 2708–2724. [CrossRef]
5. Nath, B.J.; Dehingia, K.; Sarmah, H.K. Analysis of the dynamics of a mathematical model for HIV infection. *J. Math. Comput. Sci.* **2021**, *23*, 181–195. [CrossRef]
6. Alharbi, S.A.; Rambely, A.S. A New ODE-Based Model for Tumor Cells and Immune System Competition. *Mathematics* **2020**, *8*, 1285. [CrossRef]
7. Dehingia, K.; Sarmah, H.K.; Alharbi, Y.; Hosseini, K. Mathematical analysis of a cancer model with time-delay in tumor-immune interaction and stimulation processes. *Adv. Differ. Equ.* **2021**, *2021*, 473. [CrossRef]
8. Hattaf, K.; Mohsen, A.A.; Harraq, J.; Achtaich, N. Modeling the dynamics of COVID-19 with carrier effect and environmental contamination. *Int. J. Model. Simul. Sci. Comput.* **2021**, *12*, 3. [CrossRef]
9. Lin, Q.; Zhao, S.; Gao, D.; Lou, Y.; Yang, S.; Musa, S.S.; Wang, M.H.; Cai, Y.; Wang, W.; Yang, L.; et al. A conceptual model for the coronavirus disease 2019 (COVID-19) outbreak in Wuhan, China with individual reaction and governmental action. *Int. J. Infect. Dis.* **2020**, *93*, 211–216. [CrossRef]
10. Chen, T.-M.; Rui, J.; Wang, Q.-P.; Zhao, Z.-Y.; Cui, J.-A.; Yin, L. A mathematical model for simulating the phase-based transmissibility of a novel coronavirus. *Infect. Dis. Poverty* **2020**, *9*, 1–8. [CrossRef]
11. Khan, H.; Ahmad, F.; Tunc, O.; Idrees, M. On fractal-fractional Covid-19 mathematical model. *Chaos Solit. Fractals* **2022**, *157*, 111937. [CrossRef]
12. Bushnaq, S.; Saeed, T.; Torres, D.F.; Zeb, A. Control of COVID-19 dynamics through a fractional-order model. *Alex. Eng. J.* **2021**, *60*, 3587–3592. [CrossRef]
13. Farman, M.; Akgül, A.; Nisar, K.S.; Ahmad, D.; Ahmad, A.; Kamangar, S.; Saleel, C.A. Epidemiological analysis of fractional order COVID-19 model with Mittag-Leffler kernel. *AIMS Math.* **2021**, *7*, 756–783. [CrossRef]
14. Zhang, Z.; Zeb, A.; Egbelowo, O.F.; Erturk, V.S. Dynamics of a fractional order mathematical model for COVID-19 epidemic. *Adv. Differ. Equ.* **2020**, *2020*, 420. [CrossRef]
15. Rajagopal, K.; Hasanzadeh, N.; Parastesh, F.; Hamarash, I.I.; Jafari, S.; Hussain, I. A fractional-order model for the novel coronavirus (COVID-19) outbreak. *Nonlinear Dyn.* **2020**, *101*, 711–718. [CrossRef] [PubMed]
16. Oud, M.A.A.; Ali, A.; Alrabaiah, H.; Ullah, S.; Khan, M.A.; Islam, S. A fractional order mathematical model for COVID-19 dynamics with quarantine, isolation, and environmental viral load. *Adv. Differ. Equ.* **2021**, *2021*, 106. [CrossRef]
17. Ahmad, S.W.; Sarwar, M. Fractional order model for the coronavirus (COVID-19) in Wuhan, China. *Fractals* **2022**, *30*, 2240007. [CrossRef]
18. Baleanu, D.; Mohammadi, H.; Rezapour, S. A fractional differential equation model for the COVID-19 transmission by using the Caputo-Fabrizio derivative. *Adv. Differ. Equ.* **2020**, *2020*, 299. [CrossRef]
19. Tuan, N.H.; Mohammadi, H.; Rezapour, S. A mathematical model for COVID-19 transmission by using the Caputo fractional derivative. *Chaos Solitons Fractals* **2020**, *140*, 110107. [CrossRef]
20. Li, C.; Xu, J.; Liu, J.; Zhou, Y. The within-host viral kinetics of SARS-CoV-2. *Math. Biosci. Eng.* **2020**, *17*, 2853–2861. [CrossRef]
21. Hernandez-Vargas, E.A.; Velasco-Hernandez, J.X. In-host Mathematical Modelling of COVID-19 in Humans. *Annu. Rev. Control* **2020**, *50*, 448–456. [CrossRef] [PubMed]
22. Almocera, A.E.S.; Quiroz, G.; Hernandez-Vargas, E.A. Stability analysis in COVID-19 within-host model with immune response. *Commun. Nonlinear Sci. Numer. Simul.* **2020**, *95*, 105584. [CrossRef] [PubMed]
23. Kim, K.S.; Ejima, K.; Iwanami, S.; Fujita, Y.; Ohashi, H.; Koizumi, Y.; Asai, Y.; Nakaoka, S.; Watashi, K.; Aihara, K.; et al. A quantitative model used to compare within-host SARS-CoV-2, MERS-CoV, and SARS-CoV dynamics provides insights into the pathogenesis and treatment of SARS-CoV-2. *PLoS Biol.* **2021**, *19*, e3001128. [CrossRef] [PubMed]
24. Vaidya, N.K.; Bloomquist, A.; Perelson, A.S. Modeling Within-Host Dynamics of SARS-CoV-2 Infection: A Case Study in Ferrets. *Viruses* **2021**, *13*, 1635. [CrossRef] [PubMed]
25. Yin, Y.; Xi, Y.; Xu, C.; Sun, Q. The basic reproduction number and delayed action of T cells for patients infected with SARS-CoV-2. *Mathematics* **2022**, *10*, 2017. [CrossRef]
26. Afonyushkin, V.N.; Akberdin, I.R.; Kozlova, Y.N.; Schukin, I.A.; Mironova, T.E.; Bobikova, A.S.; Cherepushkina, V.S.; Donchenko, N.A.; Poletaeva, Y.E.; Kolpakov, F.A. Multicompartmental Mathematical Model of SARS-CoV-2 Distribution in Human Organs and Their Treatment. *Mathematics* **2022**, *10*, 1925. [CrossRef]
27. Nath, B.J.; Dehingia, K.; Mishra, V.N.; Chu, Y.M.; Sarmah, H.K. Mathematical analysis of a within-host model of SARS-CoV-2. *Adv. Differ. Equ.* **2021**, *2021*, 113. [CrossRef]
28. Wang, Z.; Yang, D.; Ma, T.; Sun, N. Stability analysis for nonlinear fractional-order systems based on comparison principle. *Nonlinear Dyn.* **2014**, *75*, 387–402. [CrossRef]
29. Vargas-De-León, C. Volterra-type Lyapunov functions for fractional-order epidemic systems. *Commun. Nonlinear Sci. Numer. Simul.* **2015**, *24*, 75–85. [CrossRef]
30. Hattaf, K.; Yousfi, N. Global stability for fractional diffusion equations in biological systems. *Complexity* **2020**, *2020*, 5476842. [CrossRef]
31. dos Santos, J.P.C.; Monteiro, E.; Vieira, G.B. Global stability of fractional SIR epidemic model. *Proc. Ser. Braz. Soc. Comput. Appl. Math.* **2017**, *5*. [CrossRef]
32. Huo, J.; Zhao, H.; Zhu, L. The effect of vaccines on backward bifurcation in a fractional order HIV model. *Nonlinear Anal. Real World Appl.* **2015**, *26*, 289–305. [CrossRef]

33. Alaoui, A.L.; Tilioua, M.; Sidi Ammi, M.R.; Agarwal, P. Dynamical Analysis of a Caputo Fractional Order SIR Epidemic Model with a General Treatment Function. In *Analysis of Infectious Disease Problems (Covid-19) and Their Global Impact*; Agarwal, P., Nieto, J.J., Ruzhansky, M., Torres, D.F.M., Eds.; Infosys Science Foundation Series; Springer: Singapore, 2021. [CrossRef]
34. Ngina, P.; Mbogo, R.W.; Luboobi, L.S. Modelling optimal control of in-host HIV dynamics using different control strategies. *Comput. Math. Methods Med.* **2018**, *2018*, 9385080. [CrossRef] [PubMed]
35. Danane, J.; Meskaf, A.; Allali, K. Optimal control of a delayed hepatitis B viral infection model with HBV DNA-containing capsids and CTL immune response. *Optim. Control Appl. Methods* **2018**, *39*, 1262–1272. [CrossRef]
36. Nath, B.J.; Dehingia, K.; Sadri, K.; Sarmah, H.K.; Hosseini, K.; Park, C. Optimal control of combined antiretroviral therapies in an HIV infection model with cure rate and fusion effect. *Int. J. Biomath.* **2022**, *2022*, 2250062. [CrossRef]
37. Abdo, M.S.; Panchal, S.K.; Shah, K.; Abdeljawad, T. Existence theory and numerical analysis of three species prey–predator model under Mittag-Leffler power law. *Adv. Differ. Equ.* **2020**, *2020*, 249. [CrossRef]
38. Muthaiah, S.; Baleanu, D.; Thangaraj, N.T. Existence and Hyers-Ulam type stability results for nonlinear coupled system of Caputo-Hadamard type fractional differential equations. *AIMS Math.* **2020**, *6*, 168–194. [CrossRef]
39. Saeed, A.M.; Abdo, M.S.; Jeelani, M.B. Existence and Ulam–Hyers stability of a fractional-order coupled system in the frame of generalized Hilfer derivatives. *Mathematics* **2021**, *9*, 2543. [CrossRef]